AMD-Vol. 221/MD-VOl. 77, Mechanics of Cellulosic Materials
ASME 1997

LINEAR AND NOLINEAR MATERIAL EFFECTS ON POSTBUCKLING STRENGTH OF CORRUGATED CONTAINERS[1]

Thomas J. Urbanik

U. S. Department of Agriculture, Forest Service
Forest Products Laboratory
One Gifford Pinchot Drive
Madison, Wisconsin 53705-2398, USA
608-231-9428 Fax (608) 231-9592

ABSTRACT

Corrugated fiberboard is characterized as a nonlinear material to account for buckling phenomena prior to material breakdown and to make box compression strength more sensitive to length and width differences than allowed for by linear theory. In this report, a historical base of box compression data thought to be insensitive to length and width differences is analyzed for nonlinear material effects and compared with other data reflecting greater sensitivity. Linear material theory is shown to overpredict the strength of narrow box panels, typically the end panels, and to lead to an apparent strength equality between rectangular and square boxes of the same perimeter. Nonlinear material theory is shown to predict a lower buckling strength for low width panels and make it safer to apply box compression theory to other corrugated structures.

NOMENCLATURE

b	postbuckling constant
c	postbuckling constant
c_1, c_2	stress-strain curve constants
$\hat{c}$	normalized in-place shear modulus of elasticity
D	box depth
D_x	plate bending stiffness in machine direction
D_y	plate bending stiffness in cross-machine direction
E	modulus of elasticity
E_x	modulus of elasticity in machine direction
E_y	modulus of elasticity in cross-machine direction
$\overline{EI}_x$	beam bending stiffness in machine direction
$\overline{EI}_y$	beam bending stiffness in cross-machine direction
f	normalized buckling strain function
h	thickness
I_x, I_y	moments of inertia per unit width
k_{cr}	buckling coefficient
L	box length
l	plate width
P	box compression strength
P_{cr}	critical load of plate
P_f	failure load of plate
P_m	material edgewise compression strength
P_r	compression strength of rectangular box
P_s	compression strength of square box
P_y	yield load of plate material
S	normalized plate stiffness
U	universal plate slenderness
W	box width
Z	box perimeter
α	postbuckling constant
η	postbuckling constant
ε	strain
$\hat{\varepsilon}$	normalized buckling strain
σ	stress
σ_{cr}	average critical stress of plate
σ_f	average failure stress of plate
σ_y	material yield stress
$\hat{\sigma}, \hat{\sigma}_l, \hat{\sigma}_w$	normalized buckling stress
θ_0	nonlinear material postbuckling constant $c_1 h/P_y$
ν	geometric mean $\sqrt{\nu_1 \nu_2}$
ν_1	material Poisson's ratio for x direction
ν_2	material Poisson's ratio for y direction

[1]Supported by the Container & Kraft Paper Group of the American Forest Paper Association.

[2]The Forest Products Laboratory is maintained in cooperation with the University of Wisconsin. This article was written and prepared by U.S. Government employees on official time, and it is therefore in the public domain and nor subject to copyright.

INTRODUCTION

Knowing how to predict box compression strength from stress-strain properties of component paperboards has important implications for evaluating linerboard and corrugating medium material. A relation between box strength and paper properties according to mechanistic principles can provide the rationale to rank various paper properties by importance and manage quality control.

Theory developed at the Forest Products Laboratory (FPL) (Johnson et al., 1979; Urbanik, 1981) has previously been used to investigate the optimum mix of fiber between linerboard and medium components. Recent issues in regard to quality control practices and test methods for characterizing paper strength have raised new interest among paper makers in determining the importance of machine direction (MD) paper properties in relation to cross direction (CD) properties. Concurrent issues in box design have raised concerns about the relevance of traditional models (McKee et al., 1963) for predicting box strength of short boxes and styles different than regular slotted containers. A more mechanistic understanding of box compression behavior is needed to assess the importance of material properties.

In response to these concerns, a study was conducted between the Technical Division of the Containerboard and Kraft Paper Group (CKPG) of The American Forest & Paper Association and FPL to broaden the understanding of box compression behavior and to establish principles for experimentally verifying FPL theory. This study was conducted concurrently with a study between the CKPG and the Institute of Paper Science and Technology (lPST) to investigate experimentally how MD and CD properties of linerboard components affect box stacking performance.

OBJECTIVES AND SCOPE

The objectives of this report are (a) to relate the buckling strength of plates made of a nonlinear material to the maximum strength observed in experiments and (b) to compare the results of applying FPL nonlinear material behavior to reported data that assume linear behavior. The panels of a corrugated box and the linerboard and corrugated medium components in corrugated fiberboard are typical plate materials to which this research can be applied. The buckling theory on which this paper is based was developed in previous FPL research (Johnson and Urbanik, 1984, 1987; Urbanik, 1992). The relationship between theoretical plate buckling strength and actual maximum strength applied in this report is empirical and is treated further in a textbook by Boulson (1969). For lack of applicable data, more recent postbuckling theories of nonlinear and laminated structures (Haslach, 1991; Shin et al., 1993) were not investigated.

The motivation behind the research reported here was the inconsistency observed between existing box compression theory and unpublished industry data on how MD and CD linerboard orientation affects box compression strength. The data exhibited specimen depth and boundary condition elasticity effects found to be intractable with available theories (McKee et al.. 1963; Johnson and Urbanik, 1987). An examination of additional industry data bases revealed that principles of nonlinear material effects, box dimension effects, and boundary condition effects needed to be set forth to unify the various data

The scope of this study was limited to a broadening of postbuckling theory to include nonlinear material behavior. Data from studies by Maltenfort (1956) and McKee et al. (1963) were analyzed to compare the results of applying FPL nonlinear material behavior to reported data that had assumed linear behavior. On average, the predictive accuracy was about the same for linear and nonlinear material effects applied to the McKee data However, for those cases involving relatively high stiffness-to-strength materials or narrow box panels. nonlinear material theory proved to be superior. The significance of nonlinear material theory is further corroborated by the Maltenfort (1956) data Our results are used to show that nonlinear material theory is essential to be able to unify box compression data over a more general data base and to deal with additional effects of variations of geometry and boundary conditions.

BOX COMPRESSION MODELS

Statistical Formulae

The simplest reported box compression models have been statistical relationships between box compression strength P and box length L, width W, and depth D. The model most supported by experiments is probably the formula by Maltenfort (1956) derived from an extensive body of 14,800 compression tests. Although the original experimental design treated L and W as independent variables, there is a benefit to writing the formula in terms of the box perimeter Z and the L/W ratio as inputs. The Maltenfort formula can be put in the form

$$P = 2090 + Z\left(\frac{350}{L/W+1} + 328\right) - 237D \qquad (1)$$

where P is expressed in Newtons and D and Z in millimeters. Equation (1) is useful for examining how the strength P_r of a rectangular box compares to the strength P_s of a square box with an equal perimeter and all other variables remaining the same. The variation of the strength ratio P_r / P_s with L/W applied to the Maltenfort data (Fig. 1) predicts that treating a rectangular box as "square" leads to about a 7% strength error around L/W = 2.5.

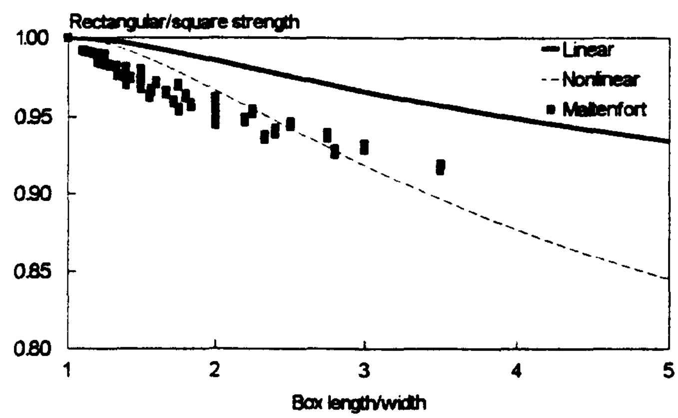

Figure 1—Ratio of strength of rectangular box to strength of square box having an equal perimeter and the same material, varying with the box length/width ratio. Points represent data from Maltenfort (1956) and curves represent two material conditions in a buckling theory. Box strength with linear material is characterized by α = 0.397 and η= 0.255 in Eq. (3). Box strength with nonlinear material is characterized by α = 0.434, η= 0.308, and θ_0 = 1.13 in Eq. (19).

Compression models advocated by other researchers predict greater errors. The formula published by Windaus et al. (1976) gives P proportional to $\sqrt{L/W}$, which predicts $P_r / P_s = 2\sqrt{L/W}\,/\,(L/W + 1)$. Podstavkina et al. (1986) made P proportional to the area-to-perimeter ratio LW/Z, which predicts $P_r / P_s = 4\,(L/W)/(L/W + 1)^2$. These formulas yield "square" approximation errors of 10% and 18% respectively, when $L/W = 2.5$. The general trends displayed by the data in figure 15 of Hoke and Gottsching (1985) also agree with the error magnitude of these statistical formulas.

Postbuckling Theory

Better strength models result from a consideration of how plates fail by buckling. If a perfectly flat plate is subjected to uniform compression in its midplane, the plate can fail by elastic or inelastic buckling. With elastic buckling, the plate remains flat until the applied stress attains a critical stress level σ_{cr}. Here the plate is considered to have buckled, but in general will not yet have collapsed As compression continues, the plate deforms laterally into a buckled shape and stress increases nonuniformly at various points around the plate. A breakdown of material eventually occurs when the local stress at some point reaches the yield stress σ_y of the material. Maximum plate strength is reached at an average applied failure stress σ_f such that $\sigma_y \geq \sigma_f \geq \sigma_{cr}$. With inelastic buckling, material breakdown occurs before the applied stress reaches σ_{cr}. The ordering of stress levels at maximum plate Strength is then $\sigma_{cr} \geq \sigma_y \geq \sigma_f$

Stress levels σ_y and σ_f can be determined experimentally. Stress σ_{cr} is a function of elastic properties and edge conditions of the plate and needs to be determined analytically. The mechanical behavior of the plate between stresses σ_{cr} and σ_f has been termed the postbuckling response. Difficulties in developing accurate theories of postbuckling behavior has led researchers (Bulson, 1969) to utilize an empirical characterization given by

$$\frac{\sigma_f}{\sigma_y} = \alpha\left(\frac{\sigma_{cr}}{\sigma_y}\right)^{\eta}; \quad \frac{\sigma_f}{\sigma_y} < 1 \tag{2}$$

in which a and η are postbuckling constants, to predict maximum plate strength. If material thickness h is considered to remain constant, Equation (2) can be rewritten in terms of load levels per unit width corresponding to the stress levels:

$$\frac{P_f}{P_y} = \alpha\left(\frac{P_{cr}}{P_y}\right)^{\eta}; \quad \frac{P_f}{P_y} < 1 \tag{3}$$

Equation (3) is more readily applicable to corrugated fiberboard wherein the corrugated material can be treated as an effective homogeneous plate.

McKee Formula-Linear Material. As noted in Bulson (1969), Equation (2) has been manipulated into various alternative forms by different researchers. The form utilized in McKee et al. (1963) for application to the panels of a corrugated box is given by

$$\frac{P_f}{P_{cr}} = c\left(\frac{P_y}{P_{cr}}\right)^{b} \tag{4}$$

in terms of new postbuckling constants, $c = \alpha$ and $b = 1 - \eta$. To apply plate theory to boxes, rectangular boxes were treated as square boxes with an equal perimeter, approximating a structure in which each supporting panel behaves identically like a simply supported plate. Only elastic buckling failure was considered. Box compression strength was then considered equal to $P_f Z$, with P_f determined from Equation (4).

Material yield strength in Equation (4) was taken to be the edgewise crush strength P_m of a short column of corrugated fiberboard. An expression for the critical load in Equation (4) was taken from March and Smith (1945) as

$$P_{cr} = k_{cr}\frac{12\sqrt{D_x D_y}}{l^2} \tag{5}$$

where l is plate width perpendicular to the direction of loading, D_x and D_y are bending stiffnesses of the corrugated fiberboard in the MD and the CD, respectively, and k_{cr} is a buckling coefficient that is an involved function of plate material properties and boundary conditions. A simplified expression for P was derived by first constructing an approximation for k_{cr} in terms of the significance of various contributing variables and with consideration for the limiting case as box depth increases. The same formula for P is more readily derived by considering the buckling strength of an infinitely long plate with compression in the direction of its length and with the unloaded edges simply supported along the length. The edge conditions beneath the loads become unimportant. For this straightforward approach, the solution for P_{cr} is obtainable from numerous textbooks on plate theory (Bulson, 1969 Ugural, 1981).

$$P_{cr} = \frac{4\pi^2\sqrt{D_x D_y}}{l^2} \tag{6}$$

Substituting Equation (6) into Equation (4). using $P_y = P_m$, $l = Z/4$, $P = P_f Z$, and rearranging terms yield

$$P = aP_m^b\left(\sqrt{D_x D_y}\right)^{1-b} Z^{2b-1} \tag{7}$$

where $a = c\,(64\pi^2)^{1-b}$. Equation (7) should be recognized as being the same as Equation (6) in the work by McKee et al. (1963).

A tit of Equation (7) to data yielded the experimental constants $a = 2.028$ and $b = 0.746$. An examination of the postbuckling response of the box panels by the more conventional Equation (2) is made by transforming a and b into $\alpha = a\,(64\pi^2)^{b-1} = 0.3942$ and $\eta = 1 - b = 0.254$. A technique advocated in Gerard (1957) and Bulson (1969) for unifying data from various sources is to plot Equation (2) with reference to the axes σ_f / σ_y and $\sqrt{\sigma_y / \sigma_{cr}}$. the second expression characterizing a universal plate slenderness U.

$$U = \sqrt{\frac{\sigma_y}{\sigma_{cr}}} = \sqrt{\frac{P_y}{P_{cr}}} \tag{8}$$

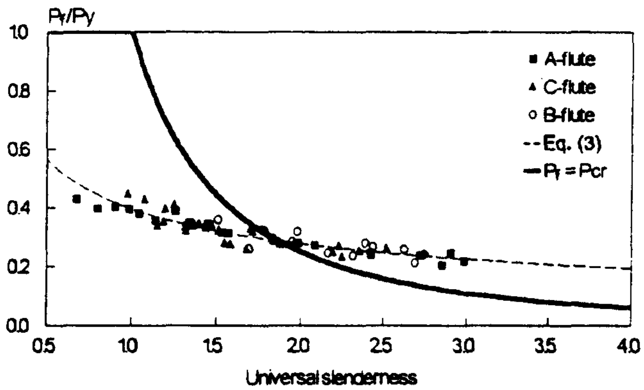

Figure 2—Variation of ratio P_f/P_y with universal slenderness U defined by Eq. (8) for supporting panels of corrugated box adjusted to an equivalent square box geometry. Points represent A-, B-, and C-flute box strength data from McKee et al. (1963). Dashed line is a fit of Eq. (3) to the data, assuming linear material behavior and failure by elastic buckling. Solid line corresponds to the condition $P_f = P_{cr}$.

Equation (3) is plotted through the McKee data in Fig. 2 following this technique. There, Equation (6) was used to determine P_{cr}. When $U > 1$, failure occurs by elastic buckling. When $U < 1$, failure occurs by inelastic buckling. Figure 2 predicts that five boxes failed by inelastic buckling and from the average value of P_f / P_y, when $U < 1$ it cart be inferred that material breakdown initiated at a value around 40% of P_m.

Bending Stiffness. Before proceeding with the introduction of nonlinear material behavior, it is important to clarify the definition of bending stiffness. In the preceding discussion, it was tacitly assumed that material behavior occurred according to the linear stress-strain law

$$\sigma = E\varepsilon \tag{9}$$

where ε is strain and E is modulus of elasticity. Subscripted moduli E_x and E_y are used here to relate to MD and CD stress–strain responses, respectively. The initial bending stiffness of a beam specimen can be determined from a conventional four-point bending test (Tappi, 1988) to be

$$\overline{EI}_x = E_x I_x = \frac{E_x h^3}{12} \quad \overline{EI}_y = E_y I_y = \frac{E_y h^3}{12} \tag{10}$$

where I_x and I_y are moments of inertia per unit width. Compared to bending of a beam, plate bending is accompanied by additional material restraint along the axis around which bending occurs. A unit width of plate is stiffer than a unit width of beam in accordance with

$$D_x = \frac{\overline{EI}_x}{1-\nu_1\nu_2} \quad D_y = \frac{\overline{EI}_y}{1-\nu_1\nu_2} \tag{11}$$

where V_1 and V_2 are material Poisson's ratios associated with x-direction and y-direction extensions, respectively. Substituting Equation (11) into Equation (7) and rearranging terms yield the equivalent expression

$$P = aP_m^b\left(\sqrt{\overline{EI}_x\,\overline{EI}_y}\right)^{1-b}(1-\nu_1\nu_2)^{b-1}Z^{2b-1} \tag{12}$$

The bending stiffness data given by McKee et al. (1963) are $\overline{EI}_x$ and $\overline{EI}_y$ values. However, these values were treated as D_x and D_y values. In essence it was assumed that $\nu_1 = \nu_2 = 0$. This approximation made sense in view of the fact that Poisson's ratios are difficult to determine for corrugated fiberboard. A recent test method (Luo et al., 1995) predicts Poisson's ratios from a combination of four-point bending tests and plate twisting tests. Values reported for an A-flute corrugated fiberboard are $\nu_1 = 0.644$ and $\nu_2 = 0.351$. With these substitutions made into Equation (12). P is predicted to be about 6.7% greater compared to when $\nu_1 = \nu_2 = 0$. Therefore, the evaluation of a using Equation (7) and letting $D_x = \overline{EI}_x$ and $D_y = \overline{EI}_y$ was inflated and reflects an average Poisson's ratio effect.

FPL Theory-Nonlinear Material. The material behavior of paper has been observed (Urbanik. 1982) to follow the stress-strain characterization given by

$$\sigma = c_1 \tanh\left(\frac{c_2}{c_1}\varepsilon\right) \tag{13}$$

where c_2 is the initial slope of the stress-strain curve and c_1 is a horizontal asymptote approached by the curve as ε increases. As the value of c_1 approaches infinity, the form of Equation (13) approaches the straight line defined by Equation (9). Equation (13) also matches the load-deformation curve of corrugated fiberboard. A cautionary remark when fitting Equation (13) to paper compression data and fiberboard compression data is that only approximate respective curves are obtained, since Equation (13) cannot be summed to yield an equal numerical form, as when adding the contributions of different paper components in a corrugated structure.

The buckling of plates with nonlinear material was considered by Johnson and Urbanik (1987). The solution is expressed in terms of a normalized buckling stress $\hat{\sigma}$ as a function of a normalized plate stiffness S given by

$$S = \frac{c_2}{c_1}\left(\frac{h}{l}\right)^2\sqrt{\frac{\nu_1}{\nu_2}} \tag{14}$$

An algorithm for determining $\hat{\sigma}$ from S is summarized in the Appendix. The critical stress σ_{cr} corresponding to $\hat{\sigma}$ is given by

$$\sigma_{cr} = c_1\hat{\sigma} \tag{15}$$

The solution of $\hat{\sigma}$ varying with S reported in Johnson and Urbanik (1987) for the case of an infinitely long, simply supported plate is repeated in Fig. 3 for various levels of the geometric mean Poisson's ratio $\nu = \sqrt{\nu_1\nu_2}$. The solution was further generalized by Urbanik (1992) to include the effect of the material in-plane shear modulus of elasticity on buckling strength.

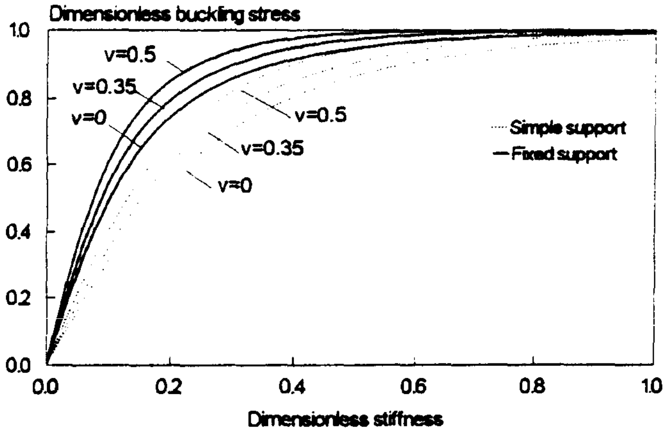

Figure 3—Variation of dimensionless buckling stress $\hat{\sigma}$ with dimensionless stiffness *S* for an infinitely long plate with nonlinear material and subjected to longitudinal compression. The buckling response for three Poisson's ratios and two support conditions is shown.

To apply the theories by Johnson and Urbanik (1987) and Urbanik (1992) to the McKee data (1963), it is helpful to restructure Equations (14) and (15) in terms of P_y, $\overline{EI}_x$, and $\overline{EI}_y$ as inputs. This is done by utilizing the theories of Johnson and Urbanik (1984) and Luo et al. (1995) that predict $v_1/v_2 = \overline{EI}_x/\overline{EI}_y$ and by recognizing that the initial slope of Equation (13) for loading in the CD yields $c_2 = E_y$. By definition $I_y = h^3/12$. Values of c_1 cannot be determined from the McKee data. However, Urbanik (1990) observed that values of c_1 reported for paper averaged about 33% greater than the corresponding values of σ_y. Therefore, a relative value of c_1 for corrugated fiberboard can be obtained by letting

$$c_1 = \theta_0 \frac{P_y}{h} \tag{16}$$

where θ_0 reflects the average ratio of $c_1 h/P_y$. Making these substitutions into Equation (14) leads to the normalized stiffness in the form

$$S = \frac{12\sqrt{\overline{EI}_x\,\overline{EI}_y}}{\theta_0 P_y l^2} \tag{17}$$

The critical load can then be determined from

$$P_{cr} = c_1\hat{\sigma}h = \theta_0 P_y \hat{\sigma} \tag{18}$$

Johnson and Urbanik (1987) showed that the initial slope of the curves for the simply supported case in Fig. 3 predicts buckling by Equation (6). In other words, for large values of θ_0 in Equation (17) or for small values of *S* a plate behaves like a linear material.

Substituting P_{cr} from Equation (18) into Equation (3) and rearranging terms yield

$$\frac{P_f}{P_y} = \alpha(\theta_0\hat{\sigma})^{\eta};\quad U > 1 \tag{19}$$

for elastic buckling of a plate with nonlinear material. Making the same substitutions into Equation (8) yields the plate slenderness

$$U = \sqrt{\frac{1}{\theta_0\hat{\sigma}}} \tag{20}$$

for nonlinear materials.

RESULTS

McKee et al. (1963) found that the prediction errors using linear material theory were independent of the specimen *L/W* ratios, which ranged from 1 to 2.9. The sensitivity to length and width effects was examined further in this study by applying Equation (4) to the box panels assuming a "square" geometry, for which $P_s = P_f Z$, for comparison with the actual "rectangular" geometry, for which $P_r = \Sigma P_f l$. Results from fitting the McKee data are given in Table 1. With linear material theory, little apparent difference is discernible. The variation of the strength ratio P_r / P_s with *L/W* is plotted in Fig. 1. The sensitivity to length and width effects inferred from linear material theory is less than that observed in the Maltenfort (1956) data (Fig. 1). McKee et al. (1963) noted this disparity, but they did not consider the maximum "square" approximation error of about 3% around *L/W* = 2.9 to be significant.

A nonlinear material model was constructed from the previous section and the Appendix and it was assumed that $P_y = P_m$ and $v = 0$, as was done previously for a linear material. The curve fitting method applied was to restructure Equation (19) in terms of *U* instead of $\hat{\sigma}$ and to search for an optimum value of θ_0 to obtain the best fit of the transformed formula

$$\log\left(\frac{P_f}{P_m}\right) = \log\alpha - 2\eta\log U(\theta_0) \tag{21}$$

applying a linear regression technique (Fig. 4). As shown in Fig. 4, the fit obtained as θ_0 approaches infinity becomes insensitive to nonlinear material effects. Results are given in Table 1 for the "square" and "rectangular" cases. The differences in the postbuckling constants obtained between these cases reflect a greater sensitivity to length and width effects compared to that

Table 1—Characterization of elastic postbuckling response

Geometry	Material character-ization	Postbuckling constants α	η	θ_0	Average error magnitude (%)
Square	Linear	0.396	0.256	∞	6.11
Rectangular	Linear	0.397	0.255	∞	6.09
Square	Nonlinear	0.421	0.295	1.30	5.84
Rectangular	Nonlinear	0.434	0.308	1.13	5.83

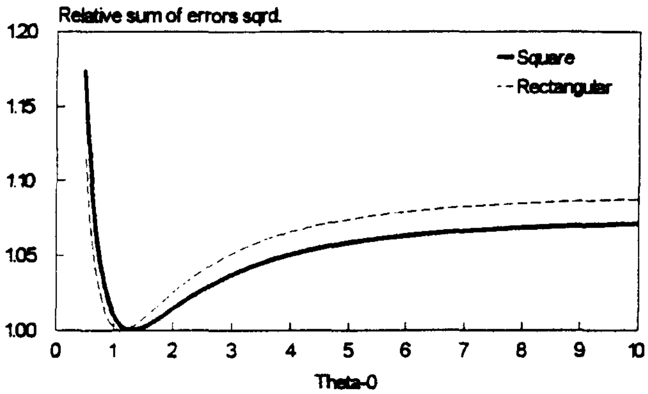

Figure 4—Sum of errors squared obtained from fitting Eq. (21) to data at various levels of θ_0. The y-axis level of each curve is scaled relative to level at optimum θ_0, which predicts the value of parameter c_1 (Eq. (16)) in a nonlinear characterization of corrugated fiberboard. As θ_0 approaches ∞, error response and predicted characterization approach the condition of linear material. Plots are shown assuming square and rectangular box geometries.

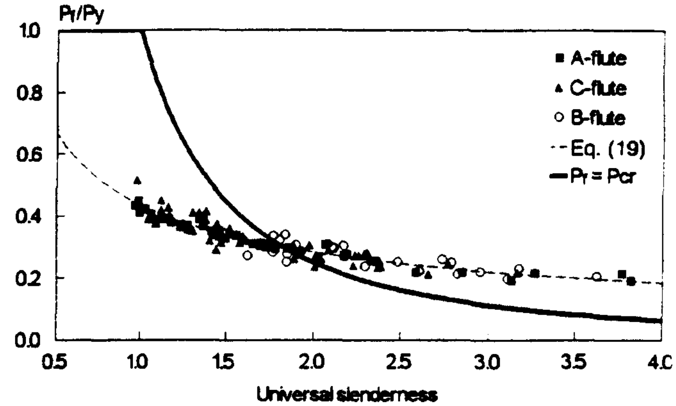

Figure 5—Variation of ratio P_f/P_y with universal slenderness U defined by Eq. (20) for supporting panels of a corrugated box. Points represent strength of A-, B-, and C-flute side and end panels scaled as the ratio 2 P_f/P of experimental box strength taken from McKee et al. (1963) Dashed line is a fit of Eq. (19) to the data, assuming nonlinear material behavior and failure by elastic buckling. Solid line corresponds to the condition $P_f = P_{cr}$.

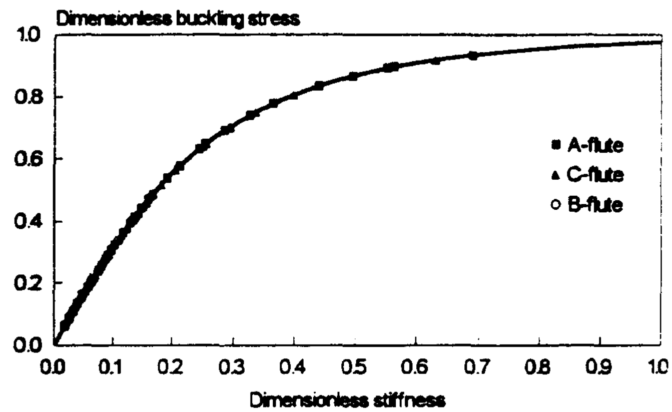

Figure 6—Predicted variation of dimensionless buckling stress $\hat{\sigma}$ with dimensionless stiffness S for panel failure of boxes in McKee et al. (1963). Points represent side and end panels from A-, B-, and C-flute boxes. Line is optimum curve through data with θ_0 = 1.13 predicted by Eq. (21). Uppermost points correspond to leftmost points in Fig. 5.

obtained with the linear material. Using a nonlinear material characterization and adding a third postbuckling constant reduced the average magnitude of the prediction error from 6.1% to 5.8%, a seemingly small improvement. However, the variation of P_r / P_s with L/W (Fig. 1), predicted by nonlinear material theory, is consistent with the data from Maltenfort (1956) and predicts greater errors up to 8% if the "square" geometry is assumed to apply.

Equation (19) is plotted through the results in Fig. 5 (nonlinear material, rectangular geometry) for comparison with Fig. 2 (linear material, square geometry). The data contain results from higher slenderness panels. reflecting the fact that using the true length dimension of the box generates greater l-values than those obtained from $Z/4$. Additionally, the low slenderness data are shifted to the right due to a reduction in material stiffness at the failure stress. The significance of a nonlinear material characterization becomes apparent by examining the variation of predicted $\hat{\sigma}$ with predicted S (Fig. 6). Most data yielded $S < 0.2$ for which linear material theory yields adequate buckling strength predictions. For the more rigid box panels, beyond $S > 0.2$, the predicted P_{cr} is significantly lower compared to predictions with linear material. The data on the right in Fig. 6 correspond to the data on the left in Fig. 5. High stiffness-to-strength, narrow box panels are most affected by nonlinear material theory.

The nonlinear material model derived from the McKee data can be expressed by rearranging Equation (19) and substituting the postbuckling evaluations from Table 1:

$$P = \sum P_m \alpha(\theta_0 \hat{\sigma})^{\eta} l = 0.9 P_m (\hat{\sigma}_l^{0.3} L + \hat{\sigma}_w^{0.3} W) \qquad (22)$$

Buckling stress values $\hat{\sigma}_l$ and $\hat{\sigma}_w$
are to be evaluated at the respective stiffness values

$$S = \frac{10.6\sqrt{\overline{EI}_x\,\overline{EI}_y}}{P_m l^2}; \quad l = L, W \qquad (21)$$

algorithm in the Appendix.

CONCLUSIONS

Characterization of corrugated fiberboard as a nonlinear material yields a more accurate account of buckling phenomonon prior to material breakdown and predicts box compression strength to be more sensitive than linear theory to length and width differences. A historical base of box compression data though to be insensitive to length and width differences was analyzed to nonlinear material effects and compared with other data reflecting greater sensitivity. A criterion for universal slenderness that increases with material edgewise crush strength and panel width and decreases with material bending stiffness was employed. Linear material theory overpredicts the strength of low slenderness box panels, typically the end panels, and leads to art apparent strength equality between rectangular and square boxes of the same perimeter. Nonlinear material theory predicts a lower buckling strength for low width panels and makes it safer to apply box compression theory to other corrugated structures. As slenderness increases the buckling response predicted by nonlinear theory approaches that of linear theory. This investigation was limited to elastic buckling failures. Additional data on the failure of box components by inelastic buckling are needed to broaden the postbuckling theory.

REFERENCES

Bulson, P.S., 1969, "The Stability of Flat Plates," American Elsevier Publishing Company, Inc., New York.

Gerard, G., 1957, "Handbook of Structural Stability. Part IV—Failure of Plates and Composite Elements," Technical Note 3784. National Advisory Commission for Aeronautics. (NACA)

Haslach, H.W. Jr., 1991, "A Tangent Modulus Theory for the Post-Buckling Behavior of Columns Made of Non-Linear Elastic Materials," Composite Material Technology, ASME, PD–Vol. 37, (January).

Hoke, U. and Gottsching, L., 1985, "Compressive Strength of Paper, Corrugated Board, and Boxes," Papier, Vol. 39, No. 10A, pp. 65–73.

Johnson, M.W., Jr., and Urbanik, T.J., 1984, "A Nonlinear Theory for Elastic Plates With Application to Characterizing Paper Properties," Journal of Applied Mechanics, Vol. 106, No. 3, pp. 146–152.

Johnson, M.W., Jr., and Urbanik, T.J., 1987, "Buckling of Axially Loaded, Long Rectangular Paperboard Plates," Wood and Fiber Science, Vol. 19, No. 2, pp. 135–146.

Johnson, M.W., Jr., Urbanik, T.J. and Denniston, W.E., 1979, "Optimum Fiber Distribution in Singlewall Corrugated Fiberboard," Research Paper FPL-RP-348, U.S. Department of Agriculture, Forest Service, Forest Products Laboratory, Madison, WI.

Luo, S., Suhling, J.C., and Laufenberg, T.L., 1995, "Bending and Twisting Tests for Measurement of the Stiffnesses of Corrugated Board," Mechanics of Cellulosic Materials, ASME, New York, AMD–Vol–209/MD–Vol. 60, pp. 91–109.

Maltenfort, G.G., 1956, "Compression Strength of Corrugated Containers," Fibre Containers, Vol. 41, No. 7.

March, H.W., and Smith, C.B., 1945, "Buckling Loads of Flat Sandwich Panels in Compression, Various Types of Edge Conditions," Report 1525, U.S. Department of Agriculture, Forest Service, Forest Products Laboratory, Madison, WI.

McKee, R.C., Gander, J.W., and Wachuta, J.R., 1963, "Compression Strength Formula for Corrugated Boxes," Paperboard Packaging (August).

Podstavkina, L.A., Zaburunova, T.A., Pluzhnikova, T.I., and Drozdova, E.G., 1986, "Effect of the Dimensions of a Box and its Inserts on Rigidity," Sb. Tr., Soversh. Tekhnol. Tarn. Kartona Kart. Tary (Rodin, V.A., et al., ed.), Moscow [Russ.], 72–87.

Shin, D.K., Griffin, O.H., Jr., and Gurdal, Z., 1993, "Postbuckling Response of Laminated Plates Under Unixial Compression," International Journal of Non-Linear Mechanics, Vol. 28, No. 1, pp. 95–115.

Tappi, 1988, "Flexural Stiffness of Corrugated Fiberboard (Mechanical Method)," UM 818.

Ugural, A.C., 1981, "Stresses in Plates and Shells," McGraw-Hill.

Urbanik, T.J., 1981, "Effect of Paperboard Stress-Strain Characteristics on Strength of Singlewall Corrugated Fiberboard: A Theoretical Approach," Research Paper FPL-RP-401, U.S. Department of Agriculture, Forest Service, Forest Products Laboratory, Madison, WI.

Urbanik, T.J., 1982, "Method Analyzes Analogue Plots of Paperboard Stress-Strain Data," Tappi, Vol. 65, No. 4, pp. 104–108.

Urbanik, T.J., 1990, "Correcting for Instrumentation With Corrugated Fiberboard Edgewise Crush Test Theory," Tappi, Vol. 73, No. 10, pp. 263–268.

Urbanik, T.J., 1992, "Effect of In-Plane Shear Modulus of Elasticity on Buckling Strength of Paperboard Plates," Wood and Fiber Science, Vol. 24, No. 4, pp. 381–384.

Windaus, G., Steinig, J., and Petermann, E., 1976, "Empirical Compilation of a Formula for the Calculation of the Compression Resistance of Folding Boxes Made of Fibreboard from the Flexural Strength Values of the Packaging Material Fibreboard and the Relevant Box Dimensions," Research and Development Laboratory of the Herzberger Paper Mill L. Osthushenrich GmbH & Co. KG, Herzberg/Harz. (Engl. trans. of Ger. title).

APPENDIX

The algorithm for determining the buckling stress of an infinitely long, simply supported plate with compression in the direction of its length and having a nonlinear material characterization is as follows:

1. Input normalized stiffness S, geometric mean Poisson's ratio, ν and dimensionless shear constant $\hat{c}$ (Urbanik, 1992). If the Poisson's ratio cannot be determined, let $\nu = 0$. If the in-plane shear modulus of elasticity cannot be determined, let $\hat{c} = 1$.
2. Define function $f(\hat{\varepsilon})$ from Johnson and Urbanik (1987), where $\hat{\varepsilon}$ is a normalized buckling strain.

$$f(\hat{\varepsilon}) = 1 - \frac{2\hat{\varepsilon}}{\sinh(2\hat{\varepsilon})} \tag{24}$$

3. Determine an initial $\hat{\varepsilon}$ from Equation (3.5′) of Urbanik (1992).

$$\hat{\varepsilon} = \frac{\pi^2 S(\hat{c}^2 + 1)^2}{12(1-\nu^2)} \tag{25}$$

4. Determine New $\hat{\varepsilon}$ from Equation (3.4′) of Urbanik (1992).

$$\text{New } \hat{\varepsilon} = \frac{\pi^2 S}{6(1-\nu^2)}\left(\hat{c} + \sqrt{1-(1-\nu^2)f(\hat{\varepsilon})}\right) \tag{26}$$

5. If New $\hat{\varepsilon} = \hat{\varepsilon}$, go to Step 7.
6. Otherwise, let $\hat{\varepsilon}$ = New $\hat{\varepsilon}$ and return to Step 4.
7. Compute the normalized buckling stress $\hat{\sigma}$ from Equation (5.1) of Johnson and Urbanik (1987).

$$\hat{\sigma} = \tanh\hat{\varepsilon} \tag{27}$$

8. Stop

AMD-Vol. 221
MD-Vol. 77

MECHANICS OF CELLULOSIC MATERIALS

– 1997 –

Presented at

THE 1997 JOINT ASME/ASCE/SES SUMMER MEETING
JUNE 29–JULY 2, 1997
EVANSTON, ILLINOIS

Sponsored by

THE APPLIED MECHANICS DIVISION, ASME
THE MATERIALS DIVISION, ASME

Edited by

RICHARD PERKINS
SYRACUSE UNIVERSITY

THE AMERICAN SOCIETY OF MECHANICAL ENGINEERS
345 East 47th Street ■ United Engineering Center ■ New York, N.Y. 10017

Statement from By-Laws: The Society shall not be responsible for statements or opinions advanced in papers. . . or printed in its publications (7.1.3)

Authorization to photocopy material for internal or personal use under circumstance not falling within the fair use provisions of the Copyright Act is granted by ASME to libraries and other users registered with the Copyright Clearance Center (CCC) Transactional Reporting Service provided that the base fee of $4.00 per page is paid directly to the CCC, 27 Congress Street, Salem MA 01970. Requests for special permission or bulk reproduction should be addressed to the ASME Technical Publishing Department.

ISBN No. 0-7918-1564-1

Library of Congress Number
97-73334

Copyright © 1997 by
THE AMERICAN SOCIETY OF MECHANICAL ENGINEERS
All Rights Reserved
Printed in U.S.A.